



## In-operando observation of microstructural evolution in a solid oxide cell electrolyte operating at high polarization

Sierra, J. X.; Poulsen, H. F.; Jørgensen, P. S.; Detlefs, C.; Cook, P.; Simons, H.; Jakobsen, A. C.; Bowen, J. R.

*Published in:*  
Journal of Power Sources

*Link to article, DOI:*  
[10.1016/j.jpowsour.2018.12.057](https://doi.org/10.1016/j.jpowsour.2018.12.057)

*Publication date:*  
2019

*Document Version*  
Peer reviewed version

[Link back to DTU Orbit](#)

### *Citation (APA):*

Sierra, J. X., Poulsen, H. F., Jørgensen, P. S., Detlefs, C., Cook, P., Simons, H., Jakobsen, A. C., & Bowen, J. R. (2019). In-operando observation of microstructural evolution in a solid oxide cell electrolyte operating at high polarization. *Journal of Power Sources*, 413, 351-359. <https://doi.org/10.1016/j.jpowsour.2018.12.057>

---

### General rights

Copyright and moral rights for the publications made accessible in the public portal are retained by the authors and/or other copyright owners and it is a condition of accessing publications that users recognise and abide by the legal requirements associated with these rights.

- Users may download and print one copy of any publication from the public portal for the purpose of private study or research.
- You may not further distribute the material or use it for any profit-making activity or commercial gain
- You may freely distribute the URL identifying the publication in the public portal

If you believe that this document breaches copyright please contact us providing details, and we will remove access to the work immediately and investigate your claim.

# Supplementary material

## S1 – Cross section of the in-operando cell

Cross section of the polished 13 $\mu\text{m}$ -ScYSZ-op cell. The top and bottom electrodes correspond to anode and cathode and platinum paste can be seen attached to electrodes. At the sides of the ScYSZ electrolyte the alumina ceramic paste can be seen.

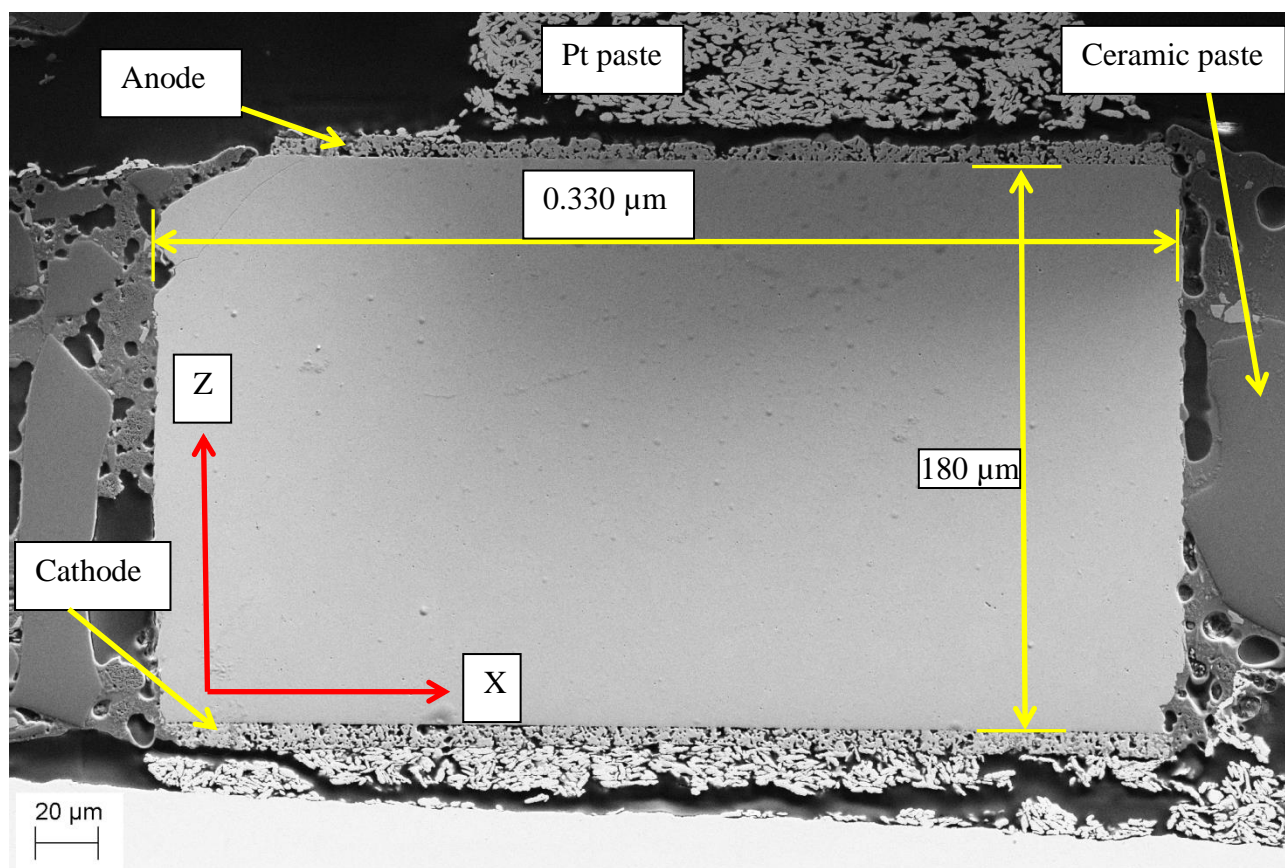


Figure S1. SEM image from a polished cross section of the cell. Directions “X” and “Z” as in beamline setup are denoted by red arrows. Vertical and horizontal dimensions are specified by text boxes next to the corresponding yellow lines delimiting the electrolyte. Yellow arrows attached to text boxes indicate the materials of the cell and cell support.

## S2 – Raw image of a section of diffraction line of ScYSZ.

An example of a near field image taken from a layer close to the anode/electrolyte region is shown in figure 1. A segment of a (111) diffraction ring can be seen, where the image was binned to 4x4 and cropped to 512x160 pixels in “y” and “z” respectively. The resulting pixel size is approximately 2.5  $\mu\text{m}$ .

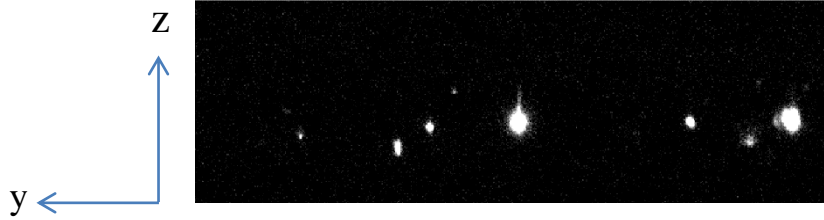


Figure S2. Near field image showing diffraction spots from ScYSZ grains at a specific layer and angle  $\omega$ , with background subtracted.

**S3 – No void formation found in as-prepared sample and cathode side of sample at operating conditions.**

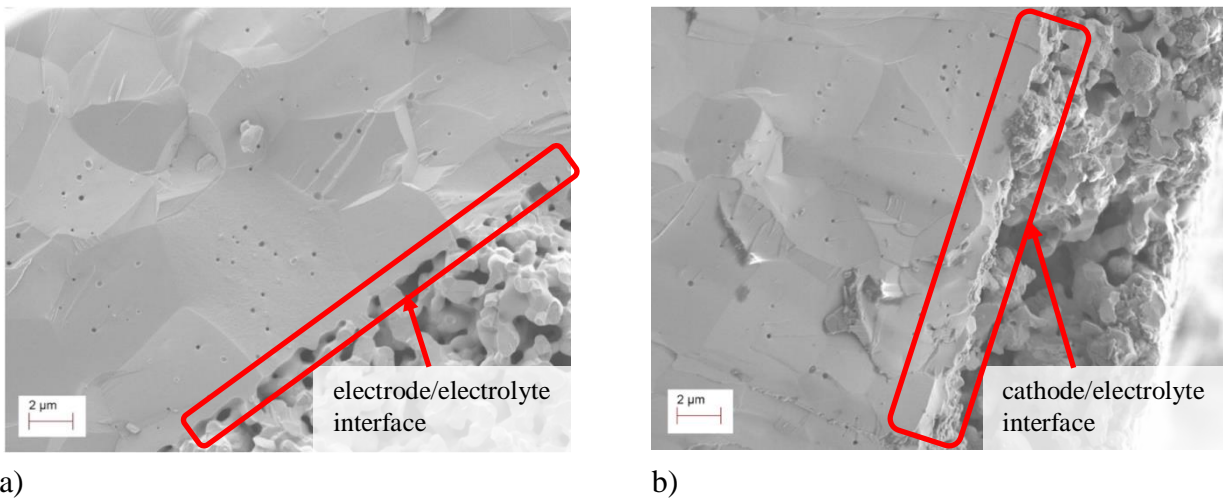
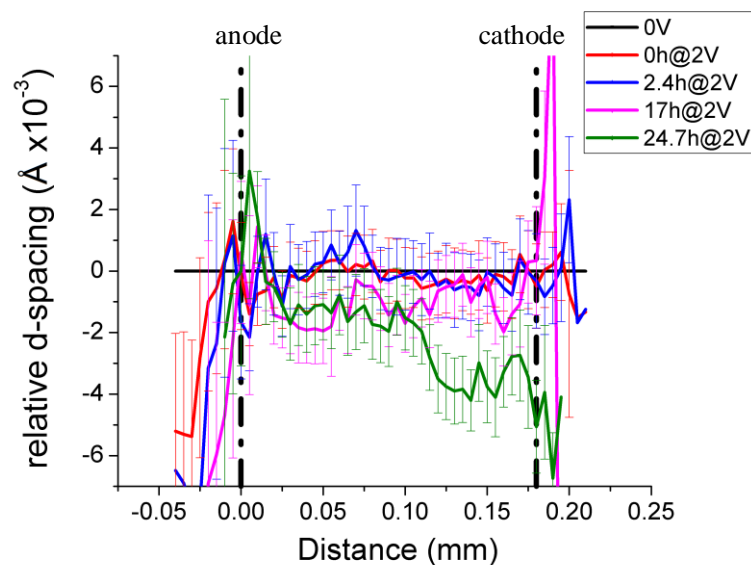


Figure S3. No void formation found in a) sample subjected to 850 °C for 72 hours without applied voltage and b) cathode/electrolyte interface of the sample subjected to 900 °C for 72 hours at 2V. All samples correspond to the 6μm-ScYSZ case and the cathode is made of LSM/YSZ. The interfaces in both cases are marked in the red rectangle.

## S4 – Relative and absolute d-spacing vs depth

The plot of d-spacing (in comparison to d-spacing at 0V) is shown in figure S4 a), where the error bars are based on the standard deviation of diffracted peak positions in the diffraction line with Miller index (111). The dashed-dotted black vertical lines delimit the anode and cathode interfaces at the left and right respectively. To determine the anode and cathode limits we use a “Number of peaks (normalize) vs depth” profile from all the stages and the known thickness of the cell in “Z”, that in this case corresponds to the “Depth” axis and it is equal to 0.180 mm, as measured by SEM from a polished cross section image, as shown in Figure S1. Figure S4 b) shows the absolute d-spacing of same stages as in a).

a)



b)

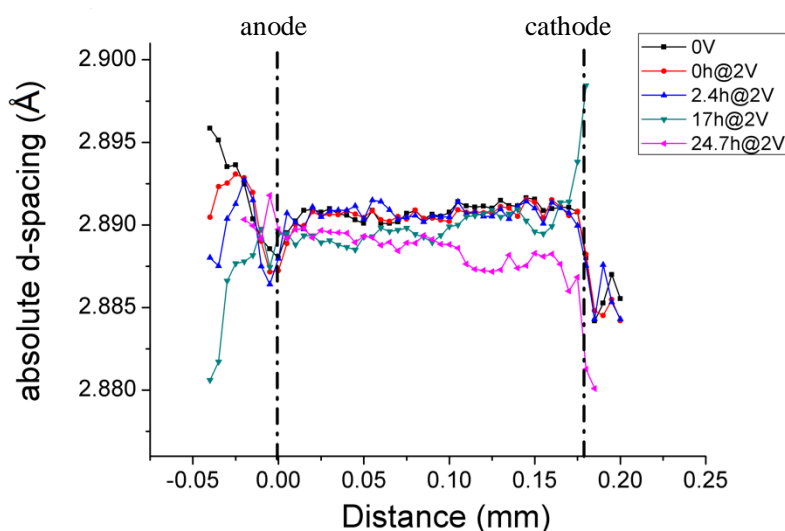


Figure S4. a) Plot of the d-spacing evolution relative to the d-spacing at 0V and high temperature including standard deviation and b) absolute d-spacing of the same stages as in a), where the average d-spacing and std. deviation of the reference sample (black line-dot) within the interfaces is  $2.8909 \pm 4 \times 10^{-4} \text{\AA}$ . Black vertical dash-dot lines at distance 0 and 0.18 mm in both figures indicate the position of the anode and cathode electrodes interfaces at left and right respectively. The legend indicates the stages described in experimental section in paper.

The number of peaks found at layers outside the dashed-dotted lines limits decrease drastically, as expected when the line beam is reaching the borders of the cell, thus we consider that the d-spacing values in electrode regions are much less reliable than the values of d-spacing in the layers corresponding to the electrolyte (inside dashed-dotted lines).

## S5 – Stress curve

The estimation of stress is based on the assumption that the change in d-spacing is only related to mechanical effects. The phase change is not analyzed here since no other diffraction lines were surveyed during in-operando experiments. The curve is estimated by a comparison to the initial time at which the voltage was applied, denoted in the paper as 0h@V.

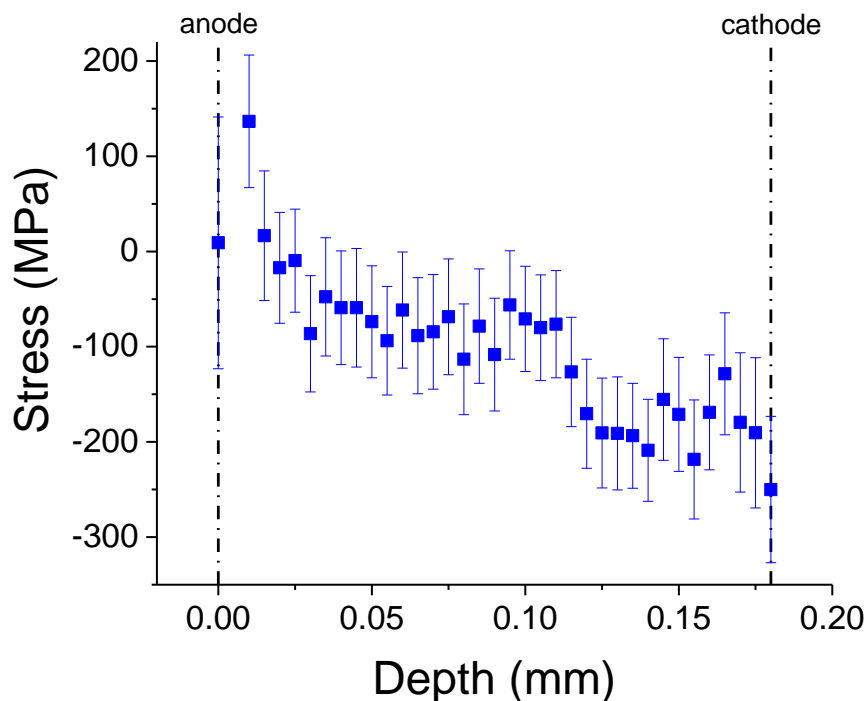


Figure S5. Expected stress across the cell after 24 hours under 2V and 700 °C, assuming that the change in d-spacing is only related to stress.

## S6 – limits of void detection

Estimation by visual inspection of the limits of void detection, using a typical image, with 10 nm pixel size. Individual voids can be seen as dark spots of minimum 2-3 pixels and forming clusters in the grain boundaries.

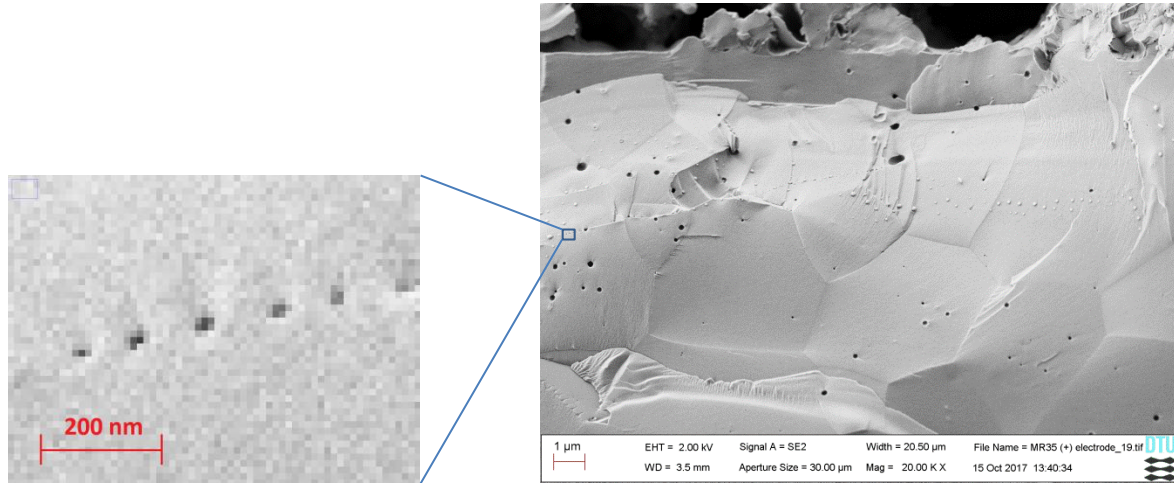


Figure S6. Limits of void detection.